C Journal of Carbon Research

MDPI

Article

A New Approach of Fabricating Graphene Nanoplates@Natural Rubber Latex Composite and Its Characteristics and Mechanical Properties

Duong Duc La [1,*], Tuan Anh Nguyen [2], Viet Do Quoc [3], Tham Thi Nguyen [2], Duy Anh Nguyen [1], Linh Nguyen Pham Duy [3], Nghia Phan Trung [3] and Sheshanath V. Bhosale [4,*]

1 Department of Inorganic Chemistry, Institute of Chemistry and Materials, Hanoi 100803, Vietnam; nguyen.duy.anh0@gmail.com (D.A.N.)
2 Advanced Nanomaterial Laboratory, Applied Nano Technology Joint Stock Company (ANTECH. Jsc), Hanoi 100803, Vietnam; Tuananhnguyendhb@gmail.com (T.A.N.); thamnt@nanoungdung.vn (T.T.N.)
3 Institute of Chemistry Technology, Hanoi University of Science and Technology, Hanoi 100803, Vietnam; vietzat@gmail.com (V.D.Q.); masterist83@gmail.com (L.N.P.D.); david@nanoungdung.vn (N.P.T.)
4 Department of Chemistry, Goa University, Goa 403206, India
* Correspondence: duc.duong.la@gmail.com (D.D.L.); svbhosale@unigoa.ac.in (S.V.B.); Tel.: +84-167-271-2734 (D.D.L.); +91-0866-960-9303 (S.V.B.)

Received: 23 July 2018; Accepted: 3 September 2018; Published: 6 September 2018

Abstract: Graphene has been demonstrated to be one of the most promising candidates to use as filler to improve the electrical, thermal, chemical and mechanical properties of natural rubber due to exceptional high surface area, superior electrical and thermal conductivity, and remarkable gas impermeability resistance. In this study, graphene nanoplates (GNPs) were mass-produced by a one-step chemical exfoliation of natural graphite and used as a filler for the fabrication of GNPs@natural rubber composite by a simple mixing method. The resultant GNPs/rubber composite was characterized by using scanning electron microscopy (SEM), and a rheometer. The prepared graphene nanoplates had a thickness of less than 10 nm and a lateral size of tens of microns. The GNPs@rubber composite revealed an exceptional improvement of abrasion loss up to seven to ten fold, along with an approximately 400%, 200% and 30% increment of elongation at break, tear strength and tensile strength, respectively. Other mechanical properties, such as hardness, compression set and rebound, as well as the effect of the GNPs loadings on the mechanical properties of the composite, were also investigated in detail.

Keywords: high-performance polymer; graphene additives; nanocomposite; rubber

1. Introduction

Rubber is one of the most commercially used polymeric matrixes mainly due to its good energy absorbing and mechanical properties. Many different rubbers have been extensively studied including, but not limited to, natural rubber, polybutadiene rubber, styrene-butadiene rubber, isobutylene isoprene rubber and poly (styrene-butadiene-styrene) rubber. Natural rubber (NR) is one of the most widely studied rubbers for practical applications such as tires, gloves, condoms and footwear, due to its biomaterial, high elasticity, cracking resistance and other superior mechanical properties [1]. However, for practical uses, like most polymers, natural rubber needs to be reinforced with fillers to improve the mechanical and physical properties, as well as enable flexibility and processability in product design and to reduce the cost of product production [2–6]. There are many types of filler that have been extensively employed to improve the properties of natural rubber, in which carbon-based

materials (carbon black, carbon fibers and carbon nanotubes), layered silicates and fibers are most commonly used to reinforce the rubber materials [7,8]. However, such high fillers usually require a high volume of loadings which results in high density, expensive composites that have poor mechanical properties [9]. Furthermore, the production of most widely used fillers of carbon black generates extensive CO_2 emissions and pollutant wastes [10].

Graphene, a two-dimensional material with exceptional chemical and physical properties, has had an extensive number of applications, such as electronic devices, energy storage and conversion, sensors, adsorption and composites [11–22]. Recently, graphene has been employed as a new type of multifunctional nanofiller to improve the mechanical properties, thermal and electrical conductivity and gas impermeability of composites [23–25]. Many graphene/natural rubber composites have been prepared by various methods, with different sources of graphene, to improve the mechanical, electrical, thermal and other properties [26,27]. For example, graphene/NR composites with excellent mechanical properties prepared by coagulation of NR latex in the presence of graphene, have been reported by Zhan and colleagues [28]. In another study, Stanier et al. reported the fabrication of graphene oxides (GO) and reduced GO (rGO) incorporated natural rubber latex nanocomposites with an increase in tensile strength of 3 MPa [29]. Potts and his colleagues also used a simple latex mixing method to disperse reduced graphene oxide in the rubber latex with enhanced mechanical, electrical and thermal properties of the rubber [30,31]. However, the majority of these graphene/rubber natural composites were fabricated by dispersing GO into NR latex, followed by reduction, which leads to a decrease in compatibility between the natural rubber and graphene due to many structural defects, the unreduced oxygen functionalities in graphene and its ability to aggregate during the in-situ reduction process. Most recently, George et al. successfully fabricated graphene dispersions, by planetary ball milling, and its NR latex nanocomposites for the first time [9]. The obtained nanocomposites showed a significant improvement in thermal conductivity, as well as electrical conductivity.

Herein, we employed our previously developed simple method for large-scale production of graphene nanoplates (GNPs) by direct chemical exfoliation of the natural graphite [32]. The obtained GNPs are incorporated in the natural rubber matrix by a simple mixing method to obtain the GNPs@rubber composite. The mechanical behaviors of the GNPs@rubber composite in comparison to bare natural rubbers are thoroughly investigated. The effects of GNPs loadings in the rubber matrix on curing characteristics and mechanical properties are also monitored.

2. Materials and Methods

2.1. Materials

Natural graphite flakes were supplied from Pressol Gmbh (Umkirch, Germany), with particle size > 100 mesh. Sodium persulfate ($Na_2S_2O_8$), Sulphuric acid (98%), acetone, ethanol (C_2H_5OH), sodium dodecyl sulfate (SDS), zinc oxide (ZnO), stearic acid, *N*-tert-butyl-2-benzothiazolesulphenamide and sulfur (S) were obtained from Xilong Chemical Co. Ltd. (Shantou, China) Natural rubber latex (NRL) containing about 60% dry rubber content (DRC) was supplied by Vietnam Rubber Latex Co., Ltd. (Binh Duong, Vietnam). Other reagents were used as received.

2.2. Fabrication of Graphene Nanoplatelets

Graphene nanoplates were synthesized by a one-step chemical exfoliation of natural graphite. Typically, 3 g of natural graphite flakes were dispersed in 240 mL of concentrated sulfuric acid by swirling for 10 min in a 1000 mL reactor. Thereafter, 18 g of sodium persulfate ($Na_2S_2O_8$) was gradually added and the reaction mixture gently stirred for 6 h at room temperature. The mixture was then filtrated directly by a glass sintered filter without quenching. The filtrated solution was separated and could be employed for the next graphite exfoliation. GNPs were rinsed with dried acetone (3 × 10 mL) and dried at 60 °C in the open air. The dried GNPs were dispersed in aqueous solution with the

assistance of SDS surfactant and sonication. The obtained GNPs-based aqueous solution was used to fabricate GNPs@natural rubber composite within 30 days following preparation.

2.3. Fabrication of GNPs@Natural Rubber Composite

GNPs/natural rubber composites were fabricated by a simple mixing method. Firstly, the natural rubber latex was mixed with various GNPs loadings of 0.3, 0.5, 0.7 and 1 phr with stirring and sonication in 6 h. Then, 60–80 mL formic acid was added dropwise to coagulate the mixture. The composite solid was cut into small pieces, washed with water to remove residual acid, and dried at 60 °C for 24 h. The GNPs@rubber pieces were vulcanized with the formulations listed in Table 1. For comparison, a reference sample of NRL was prepared using the same process but without the addition of graphene nanoplates.

Table 1. Formulations of graphene nanoplates (GNPs)/NRL composites.

Samples	Rubber	GNPs@Rubber
Compositions	100	100
ZnO	5	5
Acid Stearic	2	2
N-tert-butyl-2-benzothiazolesulphenamide	0.7	0.7
Sulfur	2.25	2.25

2.4. Sample Preparation for Measurement of Tensile and Tear Strength

The specimens were prepared by cutting the 1.00 mm thick films into a dumbbell shape with the dimensions according to ASTMD-D412-D (Standard Test Methods for Vulcanized Rubber and Thermoplastic Elastomers-Tension) for the tensile measurement. Additionally, the specimens for the tear strength measurement were prepared following ASTMD-624-C (tear sample cutting die). Prior to testing, the samples were conditioned by being placed in a climate-controlled laboratory for 24 h at a temperature of 25 ± 0.1 °C and 60 ± 5% of humidity. The cross head speed was 200 mm/min and the measurement was repeated five times for each sample. Tensile and tear strength properties of the vulcanized GNPs/rubber were determined using an INSTRON 5582 testing machine (Instron, Norwood, MA, USA).

2.5. Characterization

The crystal structures of GNPs and GNPs@natural rubber composite were characterized by scanning electron microscopy (SEM) images using an Energy dispersive X-ray (EDX)-equipped FEI Nova NanoSEM (Hillsboro, OR, USA). A BrukerAXS D8 Discover instrument (Coventry, UK) with a general area detector diffraction system (GADDS) using a Cu Kα source was utilized to obtain X-ray-diffraction (XRD) patterns. Thermal analysis was performed on the thermogravimetric analysis (TGA) instrument with a furnace and microbalance from Perkin-Elmer (Waltham, MA, USA) and operating temperature from 35 °C to 800 °C at a heating rate of 20 °C/min. X-ray photoelectron spectra (XPS) were obtained from a K-Alpha XPS instrument (Thermofisher, Waltham, MA, USA) sing monochromated aluminum as the X-ray source. Samples were vulcanized using a TOYOSEIKY Labo Plastomill 4M150 device (Tokyo, Japan). The curing properties of the composite were measured with a Toyoseiky Rotorlesss Rheometer RLR 4 (Tokyo, Japan). The wear resistance of samples was measured with Gotech GT 7012 (Gotech testing machines, Taiwan) following ASTM D5963.

3. Results and Discussion

The purity of the GNPs is demonstrated by the C 1s core level as shown in Figure 1. A survey scan of the GNPs confirmed the appearance of Na^+, sulfur and O trapped between the GNPs layers with 86% carbon, 13% oxygen, 0.7% sulfur and 0.3% sodium. The C 1s spectrum (Figure 1B) shows

only one binding energy peak at 284.5 eV, which corresponds to C–C bonds, indicating that the final product is relatively pure GNPs. The absence of peaks at 285.5 eV or 286.6 eV indicates that there is no oxidized carbon species existing in the obtained GNPs.

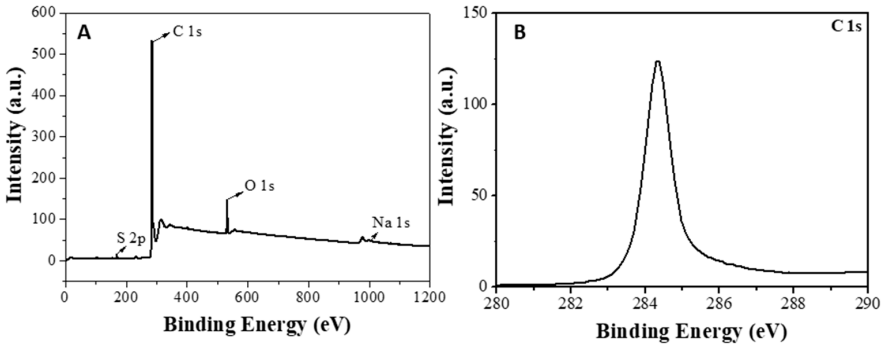

Figure 1. X-ray photoelectron spectra (XPS) of GNPs: (**A**) survey scan and (**B**) C 1s.

Figure S1A shows the Raman spectra of graphene nanoplates consists of two typical Raman bands of carbons: The D band at 1336 cm^{-1} is due to defects and disordered carbon, and the G band at 1581 cm^{-1} is used to characterize the structure of the sp^{2-} hybridized carbon atom. It is obvious that the defect-related D peak is significantly lower than the peak at the G band. In addition, a 2D peak appears at 2658 cm^{-1} of the spectra, and the number of graphene layers can be distinguished by observing the intensity ratio of the 2D and the G band peaks in the samples. It is demonstrated in the figure that the intensity of the G band is much stronger than that of the 2D band peak, corresponding to multilayered graphene. The X-ray-diffraction (XRD) analysis of the GNPs only shows a broad peak at approximately 26.5° (Figure S1B). The XRD comparison clearly shows that 002 diffraction signals of the GNPs are significantly broader and weaker compared to that of graphite flakes. These results clearly indicate that although GNPs hold multilayered flakes, the ordered interlayer structure, which are the constituent graphene layers as seen in graphite, no longer exist. The thermogravimetric analysis (TGA) data is shown in Figure S1C. Typically, the GNPs exhibit a 2.3% weight loss in the 120–230 °C temperature intervals. This weight loss is typical for graphene oxide and is attributed to the decomposition of some oxygen functionalities, along with the loss of trapped water. The weight loss of about 2% after 230 °C is attributed to the loss of intercalated H_2SO_4, Na^+, $S_2O_8{}^{2-}$ within the GNPs.

Illustrated in Figure 2A is an SEM image of the graphene nanoplates (GNPs) obtained from the facile one-step chemical exfoliation of natural graphite. It is obvious that the GNPs have a crumpled and wrinkled morphology, and are semi-transparent to the electron beam. Based on our previous study [32], one can conclude that the as-prepared GNPs have a diameter of tens of microns and a thickness of less than 10 nm. Scanning electron microscopy (SEM) was also employed to investigate the uniformness of GNPs dispersion in the natural rubber. Figure 2B shows the tensile fractured surface of the rubber, which is flat and smooth. Upon mixing with GNPs, the fractured surface of the filled rubber becomes rough with the presence of graphene nanoplates in the rubber matrix (Figure 2C and Figure S2). In the high-resolution SEM, as shown in Figure 2D, it can be clearly seen that the graphene sheets were uniformly covered by a layer of the natural rubber. The cross-section SEM image (Figure 3) of the GNPs/rubber composite also confirms the uniform distribution of GNPs in the natural rubber matrix. This result demonstrates the strong interfacial interaction between GNPs and the natural rubber [10].

First, the curing characteristics of the GNPs/natural rubber composite were evaluated to observe the rate of composite vulcanization reaction. The results are shown in Figure 4. It is obvious that effects of the GNPs on curing characteristics, in the natural rubber, are significant. At first, the torque values slightly decreased. After 1 min they started to increase to reach a maximum at the time of 3 min, and remained almost constant over time. The initial decrease was due to the softening of the composites at

the beginning of curing process and the increase was attributed to increasing crosslinking sites. While the minimum torque values are similar to the rubber samples with and without GNPs, the maximum torque of the GNPs/rubber composite is much higher than the bare natural rubber, with a value of 30 dNm compared to 25 dNm for natural rubber. These results indicate that the addition of GNPs does not affect to the processability of the rubber. Instead, it markedly improves crosslinking density, filler-matrix interactions and, therefore, enhances the mechanical properties of the composites.

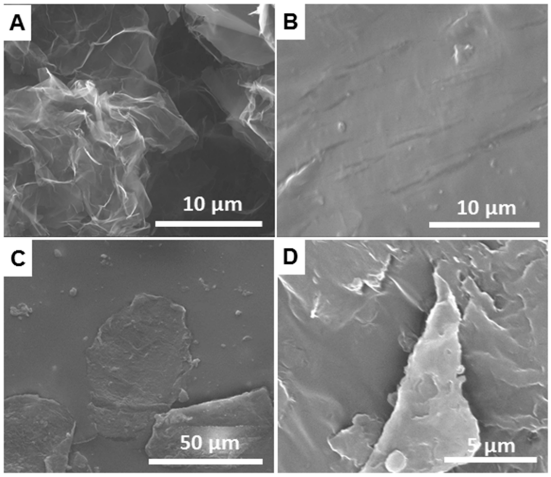

Figure 2. Scanning electron microscopy (SEM) images of (**A**) as-prepared graphene nanoplates; (**B**) unfilled natural rubber; (**C**,**D**) GNPs/natural rubber composites at 0.3 phr GNPs content.

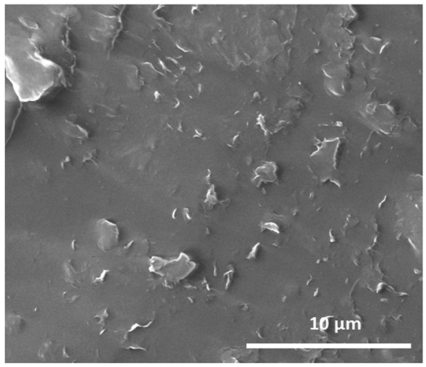

Figure 3. Cross-section SEM images of the graphene nanoplates@natural rubber latex composite.

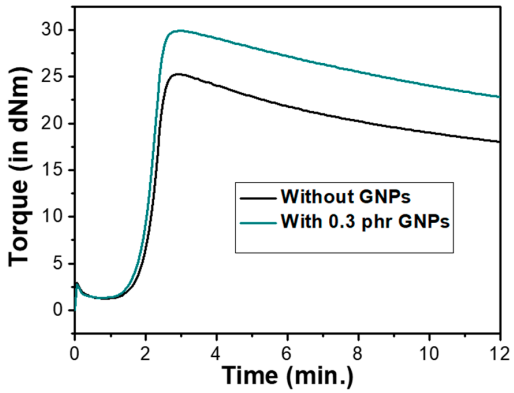

Figure 4. Torque-time curves of natural rubber composites without (black curve) and with (green curve) 0.3 phr GNPs content.

The DSC (Differential scanning calorimetry) spectra of the GNPs/rubber composite with various GNPs contents is shown in Figure S3. It is obvious that the glass transition temperature (Tg) of composite increases substantially with the increase of GNPs, which indicates an increase in hardness of the GNPs/rubber composite upon addition of GNPs. The storage module of the natural rubber with GNPs addition at various frequencies is displayed in Figure S4A. These values of the composite also increase upon the addition of GNPs. The antivibration capability of the GNPs/rubber composite was investigated by examining the dependence of tan (δ) at various frequencies with different GNPs contents (Figure S4B). The higher value of tan (δ) renders the higher antivibration capability. The highest tan (δ) was observed at the GNPs content of 0.3 phr and decreased with further addition of GNPs.

In the following section, we thoroughly investigate the enhanced mechanical performance of GNPs/natural rubber composites. Illustrated in Figure 5 are the stress-strain curves (Figure 5A) and tensile strength (Figure 5B) of the control and GNPs/natural rubber composites with different percentages of GNPs loading. It is clear that the addition of GNPs significantly enhances the tensile strength of the natural rubber latex. For example, when 0.3 phr GNPs was incorporated in the composite, an increase in tensile strength of more than 33% was obtained, compared to the control sample. The tensile strength enhancement may be ascribed to the uniform dispersion of graphene platelets in the rubber matrix, which can effectively improve the interfacial interaction and, as a result, lead to an increase in tensile strength and load transfer with the composite matrix [25]. A slight decrease in tensile strength, compared to that of 0.3 phr, was observed when the GNPs loading increased to 0.5 phr. However, it is still markedly higher than the unfilled composite with an increment of approximately 30%. Interestingly, a further increase of GNPs loading results in a significant decrease of tensile strength, even lower than the control sample. This is due to a possible agglomeration formation of GNPs [10].

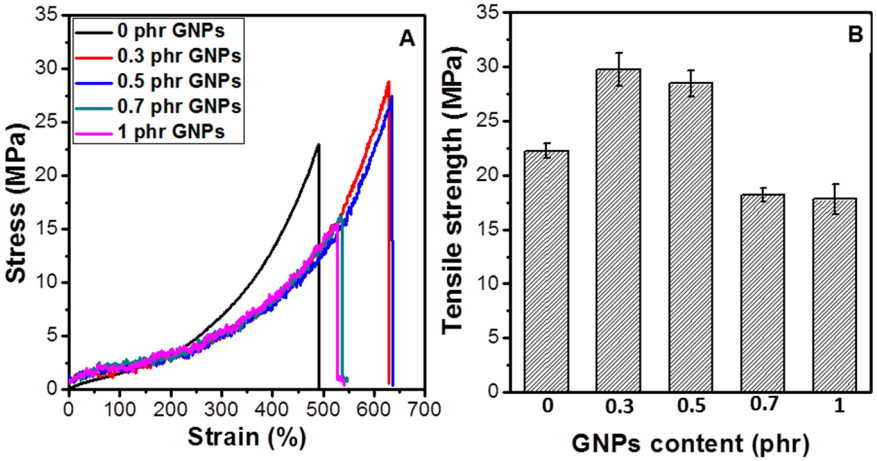

Figure 5. (**A**) Stress-strain curves of all the control samples and GNPs/natural rubber composites; (**B**) tensile strength properties of GNPs/natural rubber composites.

Figure 6A exhibits the effect of the GNPs contents on the elongation at break of the GNPs/natural rubber composites. It is clear that the elongation at break of the rubber is markedly increased upon addition of the GNPs. Trends very similar to those of the stress/strain testing were observed for the influence of the GNPs on the elongation, at break. In particular, the elongation at break increases from 5% with the control sample to nearly 20% with the addition of 0.3 phr GNPs loading. When further GNPs are introduced, the elongation at break of the composite declines, which is ascribed to the GNPs agglomeration. The addition of GNPs to the natural rubber also significantly improves the tear strength of the rubber. As shown in Figure 6B, the tear strength of the GNPs/rubber composite with 0.3% phr GNPs content is approximately 40 kN/m, compared with 22 kN/m of the control sample.

Slight decreases in tear strength are also observed when the GNPs loadings are higher than 0.3 phr. The strain induced crystallization (SIC) during the stretching process may play an important role here. This demonstrates that the addition of a small amount of GNPs facilitates the SIC of natural rubber and reaches a maximum at a GNPs content of 0.3 phr. Further increases in GNPs content, higher than 0.3 phr, leads to a change in SIC. The crosslinking density of the GNPs/rubber composite increases with the addition of GNPs. A higher crosslinking density, when GNPs exceeds 0.3 phr, leads to limited extensibility of the network chains. The lateral confinement and adsorption effect of GNPs, and the increased crosslinking density, result in reduced chain mobility of the rubber which consequently hinders the crystal lateral growth and suppresses the SIC. Therefore, the tensile strength decreases when the GNPs loading is higher than 0.3 phr.

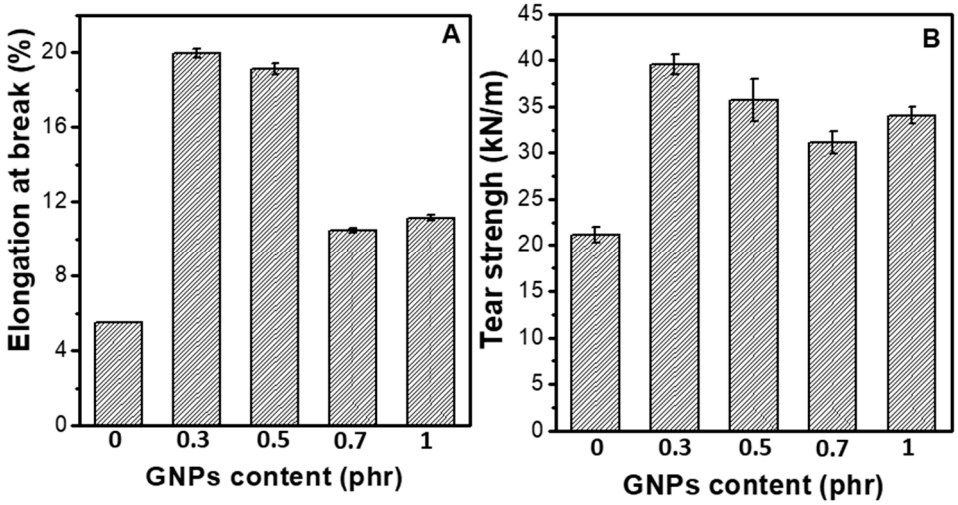

Figure 6. (**A**) Elongation at break and (**B**) tear strength of the control samples and the GNPs/natural rubber composites.

Compression set measures the ability of cured rubber to recover its original shape after a deforming force is removed, and is the ratio of elastic to viscous components of a rubber response to a given deformation. Figure 7A shows the compression set of the control sample as well as the GNP/rubber composites with different GNPs loadings. It can be seen that the compression sets of the rubber increase as a function of the GNPs loadings from 0 to 0.7 phr. However, the compression set significantly declines with a GNPs content of 1 phr. This may be ascribed to the agglomeration of the GNPs. No obvious correlation between the compression set and mechanical properties, such as tear strength, elongation at break and tensile strength, have been mentioned in previous studies [33]. Our results also confirm these earlier findings.

The use of graphene as filler for the natural rubber also improves the abrasion resistance of the composite (Figure 7B). As shown in Figure 5B, the abrasion losses of the GNPs/rubber decrease approximately 7–10 fold, compared to that of the control sample. This improvement is also due to the uniform dispersion of the GNPs in the rubber matrix, which, as a result, enhances the interfacial interaction within the rubber matrix.

The hardness and rebound properties of the GNPs/rubber composites were measured using the Shore A and Shore Rebound classification, respectively (see Figure 8). It can be clearly seen in Figure 8A,B that the improvements in hardness and rebound of the natural rubber with the addition of the GNPs were negligible, which is a maximum 10% increment in both hardness and rebound with 0.3 phr GNPs loading. This is because, unlike other fillers such as carbon particles, which commonly increase the hardness of the rubber, the graphene with two dimensions tends to be flexible and does not significantly affect the hardness of the rubber.

The mechanical properties of the GNPs/natural rubber composite at various GNPs contents is summarized in Table 2, and a comparison with other studies on graphene/rubber composite is displayed in Table 3.

It is apparent from Table 3, that even with a low content of graphene, the mechanical properties of GNP/rubber composite significantly increased in this study, which is equivalent to the reports on these composites in other studies.

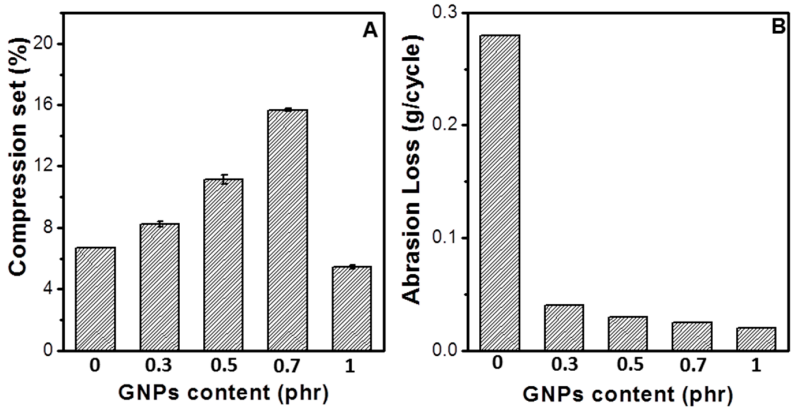

Figure 7. (**A**) Compression set and (**B**) abrasion loss of the control samples and the GNPs/natural rubber composites.

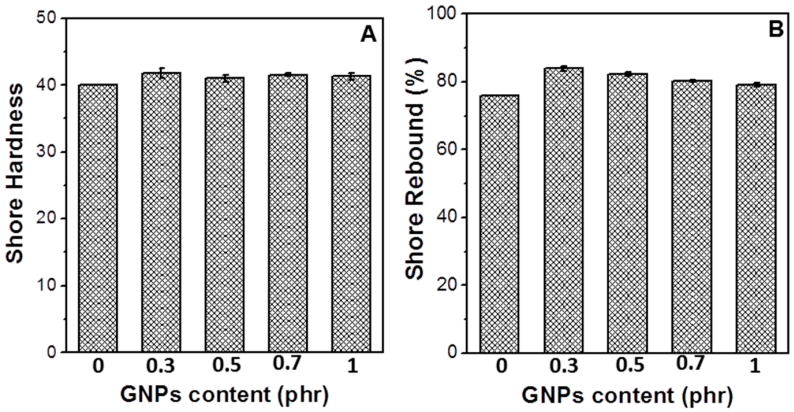

Figure 8. (**A**) Shore hardness and (**B**) shore rebound of the control samples and the GNPs/natural rubber composites.

Table 2. A summary of the mechanical properties of the GNPs/natural rubber composite.

Properties \ GNPs Content, phr	0	0.3	0.5	0.7	1
Stress at 300% elongation, MPa	7	5	5	5	5
Strain at break, %	22.5	30.0	29.2	18.3	17.9
Tensile strength, MPa	22.2	29.5	28.3	18.2	17.6
Elongation at break, %	5.64	19.60	18.82	10.43	11.21
Tear strength, kN/m	21.3	39.5	35.5	31.2	33.6
Compression set, %	6.72	8.45	11.33	15.81	5.24
Abrasion loss, g/cycle	0.280	0.041	0.031	0.025	0.021
Shore hardness, phr	40.0	41.9	40.6	41.3	41.3
Shore rebound, %	76.92	48.62	82.05	80.77	80.77

Table 3. A comparison with other studies on graphene/rubber composite.

Graphene Contents (phr)	Abrasion Loss, g/Cycle	Stress at 300% Elongation, MPa	Strain at Break, %	Tensile Strength, MPa	Elongation at Break, %	Shore Hardness, phr	Reference
2	-	-	-	20	-	-	[10]
25	-	break	-	9.2	260	69.7	[34]
5	-	1.28	8.96	10.5	-	-	[31]
0.3	0.041	5	30.0	29.5	19.60	41.9	This study

4. Conclusions

In short, we have employed a one-step approach for the mass production of high-quality graphene nanoplates, 10 nm in thickness and tens of microns in lateral size. The prepared GNPs are uniformly dispersed in the natural rubber matrix of the GNPs/rubber composite at as low as 0.3 phr content. With reinforcement of the GNPs, the abrasion of the composite decreases 7 to 10 times in comparison to the bare natural rubber. Furthermore, the GNPs also significantly enhances the elongation at break, tear strength and tensile strength with 400%, 200%, and 30% increments, respectively. The addition of GNPs also increases the max torque and compression set, decreases both the abrasion loss as well as the effect on the hardness and rebound properties. This use of a new, high-quality source of graphene to reinforce natural rubber, will certainly advance the field, one step closer, towards the practical application of graphene to improve the mechanical properties of composites.

Supplementary Materials: The following are available online at http://www.mdpi.com/2311-5629/4/3/50/s1, Figure S1: (a) Raman spectrum; (B) X-ray diffraction XRD pattern and (C) Thermogravimetric analysis TGA spectrum of graphene nanoplatelets; Figure S2: SEM images of the graphene nanoplates@natural rubber latex composite; Figure S3: Differential scanning calorimetry (DSC) spectrum of the natural rubber and GNPs/rubber composite. Differential scanning calorimetry (purple line) and scanning calorimetry (blue line); Figure S4: Dynamic mechanical analysis (DMA) spectra: (A) Storage module and (B) tan (δ) of GNPs/rubber composites with various GNPs contents. 0.3 phr (blue line), 0.5 phr (pink line), 0.7 phr (green line), 1 phr (orange line).

Author Contributions: D.D.L. and T.A.N. performed all the experiments and V.Q.D., T.T.N., L.N.P.D. and N.P.T. helped with SEM, Stress-strain and torque curve analysis, D.A.N. helped with XRD, TGA, DMA and DSC; D.D.L. and S.V.B. (IICT) monitored the analysis, D.D.L and S.V.B. supervised the research project. All the co-authors contributed to the manuscript preparation.

Funding: This work was financially supported by the Advanced Nanomaterials Lab (AN Lab).

Acknowledgments: The authors acknowledge the facilities, and the scientific and technical assistance, of the Australian Microscopy & Microanalysis Research Facility at RMIT University and Institute of Materials and Chemistry. S.V.B. acknowledges University Grant Commission (UGC)—Faculty Research Program (India) for providing financial support and an award of professorship.

Conflicts of Interest: The authors declare no conflicts of interest.

References

1. Ahmed, K.; Nizami, S.S.; Raza, Z.N.; Mahmood, K. Effect of micro-sized marble sludge on physical properties of natural rubber composites. *Chem. Ind. Chem. Eng. Q.* **2013**, *19*, 281–293. [CrossRef]
2. Moniruzzaman, M.; Winey, K.I. Polymer nanocomposites containing carbon nanotubes. *Macromolecules* **2006**, *39*, 5194–5205. [CrossRef]
3. Fahim, I.S.; Elhaggar, S.M.; Elayat, H. Experimental investigation of natural fiber reinforced polymers. *Mater. Sci. Appl.* **2012**, *3*, 59–66. [CrossRef]
4. Gangopadhyay, R.; De, A. Conducting polymer nanocomposites: A brief overview. *Chem. Mater.* **2000**, *12*, 608–622. [CrossRef]
5. Bryning, M.B.; Islam, M.F.; Kikkawa, J.M.; Yodh, A.G. Very low conductivity threshold in bulk isotropic single-walled carbon nanotube-epoxy composites. *Adv. Mater.* **2005**, *17*, 1186–1191. [CrossRef]
6. Rajan, V.; Dierkes, W.K.; Joseph, R.; Noordermeer, J.W. Science and technology of rubber reclamation with special attention to NR-based waste latex products. *Prog. Polym. Sci.* **2006**, *31*, 811–834. [CrossRef]
7. Peng, Z.; Kong, L.X.; Li, S.-D.; Chen, Y.; Huang, M.F. Self-assembled natural rubber/silica nanocomposites: Its preparation and characterization. *Compos. Sci. Technol.* **2007**, *67*, 3130–3139. [CrossRef]

8. Peng, Z.; Feng, C.; Luo, Y.; Li, Y.; Kong, L. Self-assembled natural rubber/multi-walled carbon nanotube composites using latex compounding techniques. *Carbon* **2010**, *48*, 4497–4503. [CrossRef]
9. George, G.; Sisupal, S.B.; Tomy, T.; Pottammal, B.A.; Kumaran, A.; Suvekbala, V.; Gopimohan, R.; Sivaram, S.; Ragupathy, L. Thermally conductive thin films derived from defect free graphene-natural rubber latex nanocomposite: Preparation and properties. *Carbon* **2017**, *119*, 527–534. [CrossRef] [PubMed]
10. Kang, H.; Tang, Y.; Yao, L.; Yang, F.; Fang, Q.; Hui, D. Fabrication of graphene/natural rubber nanocomposites with high dynamic properties through convenient mechanical mixing. *Compos. Part B Eng.* **2017**, *112*, 1–7. [CrossRef]
11. Novoselov, K.S.; Geim, A.K.; Morozov, S.; Jiang, D.; Zhang, Y.; Dubonos, S.A.; Grigorieva, I.; Firsov, A. Electric field effect in atomically thin carbon films. *Science* **2004**, *306*, 666–669. [CrossRef] [PubMed]
12. Bunch, J.S.; Van Der Zande, A.M.; Verbridge, S.S.; Frank, I.W.; Tanenbaum, D.M.; Parpia, J.M.; Craighead, H.G.; McEuen, P.L. Electromechanical resonators from graphene sheets. *Science* **2007**, *315*, 490–493. [CrossRef] [PubMed]
13. Katsnelson, M.I. Graphene: Carbon in two dimensions. *Mater. Today* **2007**, *10*, 20–27. [CrossRef]
14. Kopelevich, Y.; Esquinazi, P. Graphene physics in graphite. *Adv. Mater.* **2007**, *19*, 4559–4563. [CrossRef]
15. Morozov, S.; Novoselov, K.; Katsnelson, M.; Schedin, F.; Elias, D.; Jaszczak, J.; Geim, A. Giant intrinsic carrier mobilities in graphene and its bilayer. *Phys. Rev. Lett.* **2008**, *100*, 016602. [CrossRef] [PubMed]
16. Becerril, H.A.; Mao, J.; Liu, Z.; Stoltenberg, R.M.; Bao, Z.; Chen, Y. Evaluation of solution-processed reduced graphene oxide films as transparent conductors. *ACS Nano* **2008**, *2*, 463–470. [CrossRef] [PubMed]
17. La, D.D.; Rananaware, A.; Salimimarand, M.; Bhosale, S.V. Well-dispersed assembled porphyrin nanorods on graphene for the enhanced photocatalytic performance. *ChemistrySelect* **2016**, *1*, 4430–4434. [CrossRef]
18. La, D.D.; Hangarge, R.V.; Bhosale, S.V.; Ninh, H.D.; Jones, L.A.; Bhosale, S.V. Arginine-Mediated Self-Assembly of Porphyrin on Graphene: A Photocatalyst for Degradation of Dyes. *Appl. Sci.* **2017**, *7*, 643. [CrossRef]
19. La, D.D.; Nguyen, T.A.; Jones, L.A.; Bhosale, S.V. Graphene-Supported Spinel $CuFe_2O_4$ Composites: Novel adsorbents for arsenic removal in aqueous media. *Sensors* **2017**, *17*, 1292. [CrossRef] [PubMed]
20. La, D.D.; Bhosale, S.V.; Jones, L.A.; Revaprasadu, N.; Bhosale, S.V. Fabrication of a Graphene@TiO2@ Porphyrin hybrid material and its photocatalytic properties under simulated sunlight irradiation. *ChemistrySelect* **2017**, *2*, 3329–3333. [CrossRef]
21. La, D.D.; Thi, H.P.N.; Nguyen, T.A.; Bhosale, S. Effective removal of Pb (II) using Graphene@Ternary oxides composite as adsorbent in aqueous media. *New J. Chem.* **2017**, *41*, 14627–14634. [CrossRef]
22. La, D.D.; Patwari, J.M.; Jones, L.A.; Antolasic, F.; Bhosale, S.V. Fabrication of a GNP/Fe–Mg Binary Oxide Composite for Effective Removal of Arsenic from Aqueous Solution. *ACS Omega* **2017**, *2*, 218–226. [CrossRef]
23. Geim, A.K.; Novoselov, K.S. The rise of graphene. *Nat. Mater.* **2007**, *6*, 183–191. [CrossRef] [PubMed]
24. Xing, W.; Wu, J.; Huang, G.; Li, H.; Tang, M.; Fu, X. Enhanced mechanical properties of graphene/natural rubber nanocomposites at low content. *Polym. Int.* **2014**, *63*, 1674–1681. [CrossRef]
25. Rafiee, M.A.; Rafiee, J.; Wang, Z.; Song, H.; Yu, Z.-Z.; Koratkar, N. Enhanced mechanical properties of nanocomposites at low graphene content. *ACS Nano* **2009**, *3*, 3884–3890. [CrossRef] [PubMed]
26. Stankovich, S.; Dikin, D.A.; Dommett, G.H.; Kohlhaas, K.M.; Zimney, E.J.; Stach, E.A.; Piner, R.D.; Nguyen, S.T.; Ruoff, R.S. Graphene-based composite materials. *Nature* **2006**, *442*, 282–286. [CrossRef] [PubMed]
27. Korattanawittaya, S.; Petcharoen, K.; Sangwan, W.; Tangboriboon, N.; Wattanakul, K.; Sirivat, A. Durable compliant electrode based on graphene and natural rubber. *Polym. Eng. Sci.* **2017**, *57*, 129–136. [CrossRef]
28. Zhan, Y.; Wu, J.; Xia, H.; Yan, N.; Fei, G.; Yuan, G. Dispersion and exfoliation of graphene in rubber by an Ultrasonically-Assisted latex mixing and in situ reduction process. *Macromol. Mater. Eng.* **2011**, *296*, 590–602. [CrossRef]
29. Stanier, D.; Patil, A.; Sriwong, C.; Rahatekar, S.; Ciambella, J. The reinforcement effect of exfoliated graphene oxide nanoplatelets on the mechanical and viscoelastic properties of natural rubber. *Compos. Sci. Technol.* **2014**, *95*, 59–66. [CrossRef]
30. Potts, J.R.; Shankar, O.; Du, L.; Ruoff, R.S. Processing-morphology-property relationships and composite theory analysis of reduced graphene oxide/natural rubber nanocomposites. *Macromolecules* **2012**, *45*, 6045–6055. [CrossRef]

31. Potts, J.R.; Shankar, O.; Murali, S.; Du, L.; Ruoff, R.S. Latex and two-roll mill processing of thermally-exfoliated graphite oxide/natural rubber nanocomposites. *Compos. Sci. Technol.* **2013**, *74*, 166–172. [CrossRef]
32. La, M.D.D.; Bhargava, S.; Bhosale, S.V. Improved and a simple approach for mass production of graphene nanoplatelets material. *ChemistrySelect* **2016**, *1*, 949–952. [CrossRef]
33. Movahed, S.O.; Ansarifar, A.; Mirzaie, F. Effect of various efficient vulcanization cure systems on the compression set of a nitrile rubber filled with different fillers. *J. Appl. Polym. Sci.* **2015**, *132*, 41512. [CrossRef]
34. Schopp, S.; Thomann, R.; Ratzsch, K.F.; Kerling, S.; Altstädt, V.; Mülhaupt, R. Functionalized graphene and carbon materials as components of Styrene-Butadiene rubber nanocomposites prepared by aqueous dispersion blending. *Macromol. Mater. Eng.* **2014**, *299*, 319–329. [CrossRef]